

Stem volume retrieval in boreal forests from ERS-1/2 interferometry

Maurizio Santoro^{a,*}, Jan Askne^{a,1}, Gary Smith^{a,1}, Johan E.S. Fransson^{b,2}

^aDepartment of Radio and Space Science, Chalmers University of Technology, S-412 96, Gothenburg, Sweden

^bDepartment of Forest Resource Management and Geomatics, Swedish University of Agricultural Sciences, S-901 83, Umeå, Sweden

Received 16 May 2001; received in revised form 15 October 2001; accepted 15 October 2001

Abstract

C-band repeat-pass interferometry, in particular, the coherence, has been shown to be of great potential for stem volume retrieval. For boreal forests, we have investigated a stem volume retrieval method based on inversion of ERS-1/2 coherence measurements by means of a semiempirical model. A multitemporal combination of several stem volume estimates has been used in order to reduce errors in the estimation. The retrieval procedure was first applied in a forest estate located in Kättböle, Sweden, where accurate in situ measurements were taken. Stem volume was determined both at the stand level (between 2 and 14 ha) and at the pixel level (25 × 25 m). A multitemporal combination of coherence data acquired in stable winter-type conditions gave the most accurate results. Based on the results obtained in Kättböle, the retrieval procedure was extended to a large area of 4235 km² around Kättböle. Retrieval was performed in all forested areas on a pixel basis (25 × 25 m), generating stem volume maps. In Kättböle, at the stand level, stem volume up to 350 m³/ha was estimated with an error comparable to the ground truth, i.e. 10 m³/ha. At the pixel level, the error reached the value of 55 and 71 m³/ha in the forest estate and in the large area, respectively. Compared to the results from the stand analysis, the higher error is believed to be mainly due to the higher uncertainty of coherence estimation at high stem volume and to geometric mismatch between field data and coherence data. Moreover, over large areas, spatial variation of the parameters in the model should be considered. © 2002 Elsevier Science Inc. All rights reserved.

Keywords: SAR interferometry; Coherence; Stem volume retrieval; Multitemporal approach

1. Introduction

Boreal forests represent one of the largest biomes on Earth, covering ca. 18% of its surface. They constitute a broad belt of vegetation at the northern latitudes of the American and the Eurasian continents. These are one of the less inhabited and more remote areas of the globe, and little attention has been paid in the past to their conditions. Nevertheless, during the last decades, the attention on boreal forests has increased because of their environmental and economic role. Global warming, due to an increase of greenhouse gases in the atmosphere, has been shown to have an effect particularly in the northern regions, affecting the vegetation in terms of yearly life cycle, growth, and extent. Boreal forests represent one of the major carbon

sinks on Earth; therefore, they are fundamental for carbon uptake from the atmosphere, thus reducing the amount of greenhouse gases. Finally, the high consumption of wood as primary material for several purposes implies a massive trade of forest products, which represent one of the main sources of income in Canada, Russia, and the Scandinavian countries. Forest monitoring on a regular basis has therefore to be carried out, and accurate inventory is needed to measure the quantity of wood available on a large scale.

Remote sensing can deal with these requirements. The amount of data from airborne and spaceborne sensors operating at several frequencies has been shown to provide much information for forestry applications. Compared to optical and infrared instruments, synthetic aperture radar (SAR) has the advantage to provide image acquisition, independently of darkness and weather conditions. In particular, spaceborne SAR is able to cover large areas (of the order of thousands of square kilometers) with a reasonable resolution and to acquire data of any part of the Earth on a periodical basis. This becomes useful for forest monitoring, especially in areas that are scarcely populated or difficult to reach.

* Corresponding author. Fax: +46-31-772-18-84.

E-mail addresses: santoro@rss.chalmers.se (M. Santoro), askne@rss.chalmers.se (J. Askne), smith@rss.chalmers.se (G. Smith), johan.fransson@resgeom.slu.se (J.E.S. Fransson).

¹ Fax: +46-31-772-18-84.

² Fax: +46-90-14-19-15.

Several authors have investigated the possibility to retrieve values of biophysical parameters (i.e. quantities characterising forested areas such as tree height, age, stem volume or biomass, etc.) using spaceborne SAR imagery acquired at the C-band. Simple or more structured models relating the SAR backscatter to forest parameters have been developed and inverted to estimate the parameters from SAR data (Dobson et al., 1995; Pulliainen, Heiska, Hyypä, & Hallikainen, 1994). Because of the short wavelength, saturation of the backscatter occurs at relatively low stem volume, thus strongly limiting the retrieval (Fransson & Israelsson, 1999; Pulliainen, Mikkilä, Hallikainen, & Ikonen, 1996). Nevertheless, when stem volume estimates from several images have been combined in a multitemporal fashion, the retrieval accuracy for stands of at least 5 ha could be improved (Kurvonen, Pulliainen, & Hallikainen, 1999).

The availability of imagery acquired over the same area in different times has given rise to repeat-pass SAR interferometry (InSAR), a technique that measures the correlation between two images acquired from two slightly separated positions. The degree of correlation, from now onwards referred to as coherence, is generally low over forests because of the low temporal stability of trees; in particular, it has been shown that coherence decreases for increasing stem volume (Askne & Smith, 1996), or age (Floury, Le Toan, & Souyris, 1996). According to Castel, Martinez, Beaudoin, Wegmüller, and Strozzi (2000), Martinez, Beaudoin, Wegmüller, Le Toan, and Strozzi (1998) and Smith, Dammert, and Askne (1996), several factors such as time span between image acquisition, weather conditions, baseline, and topography affect the decorrelation.

When coherence has been related to stem volume, regression methods or modelling have been used. For boreal forests, Fransson, Smith, Askne, and Olsson (2001) and Smith et al. (1998) have shown that a linear regression can relate coherence to stem volume, even though some saturation effects have been noticed at high stem volumes in specific cases. Wagner et al. (2000) used exponential functions and statistically derived coefficients instead. A semiempirical model, the Interferometric Water Cloud Model (IWCM), was introduced by Askne, Dammert, Fransson, Israelsson, and Ulander (1995), taking into account the scattering of the radio waves by the forest and the InSAR geometry. A simpler empirical model to describe forest coherence was presented in Koskinen, Pulliainen, Hyypä, Engdahl, and Hallikainen (2001).

For the same area, retrieval of stem volume has been performed in Fransson et al. (2001), using a linear regression, and in Santoro, Askne, Dammert, Fransson, and Smith (1999) from the IWCM. The retrieval accuracy depended on the meteorology at acquisition, as well as on the ground truth and the tree species, reaching the order of 30 m³/ha when the ground was covered with snow. A comparison of retrieval accuracy from several spaceborne techniques (optical and radar based) has been conducted in

Hyypä et al. (2000), showing that ERS coherence has the highest potential of current satellite sensors for forestry inventory applications.

In this work, the accuracy of stem volume retrieval from a relatively extensive InSAR data set is analysed. Firstly, semiempirical models that relate coherence and backscatter to stem volume are trained and inverted on a forest estate, characterised by accurate in situ data. Retrieval from a single image and from a multitemporal combination of estimated values is performed. Results are obtained both at the stand level and on a pixel basis; they are compared to ground truth data, and the retrieval accuracy is computed. Based on the results obtained at the local site, the retrieval procedure is extended to a large forested area surrounding the forest estate. Stem volume maps are generated, and the estimated are values compared at the pixel level to the available ground truth data.

2. Test site and data set

2.1. Test sites

In this work, we focus on a small site located near Kättböle (60°N 17°E) and on forested areas among the provinces of Uppland and Västmanland, northwest of Stockholm, Sweden. Kättböle is a forest estate covering 550 ha, with relatively flat topography where elevation ranges between 75 and 110 m above sea level. Boreal coniferous species such as Scots pine (*Pinus sylvestris*) and Norway spruce (*Picea abies*) dominate even though some broad-leaf trees, the commonest being birch (*Betula pendula*), are also present. The dominant soil type is till with a field layer consisting mainly of blueberry (*Vaccinium myrtillus*) and cowberry (*Vaccinium vitis-idaea*). The approximate extent of the large forested area is shown in Fig. 1. The whole area is rather flat; the maximum altitude above sea level is about 150 m.

2.2. Ground truth data

In Scandinavia, the common measure used for forest inventory is stem volume. Stem volume is measured in cubic meters per hectare and represents the volume of tree trunks per area unit, including bark but excluding branches and stumps. It can be converted into the approximate total above-ground dry biomass of trees in tons per ha using a scaling factor of 0.6 (Häme, Salli, & Lahti, 1992). The basic unit for forest inventory is a sample plot with a 5–10-m radius or a relascope point, where measurements related to site conditions, tree dimensions, and species are collected. Plots are arranged in square or rectangular clusters; these have a size and a distribution specific to the kind of investigation that needs to be performed (large-scale or detailed inventory, geostatistic studies, etc.). Plot-wise measurements are used to estimate forest properties at

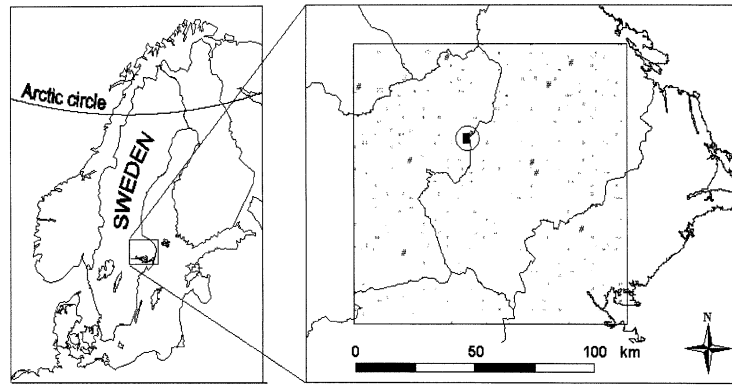


Fig. 1. Map of Sweden (left) and zoom of the investigated area (right). In this picture, the box delimits the large area. The circle includes the Kättböle site, located on the border between the provinces of Västmanland (left) and Uppland (right). The dots represent positions of NFI plots in the area. SMHI weather stations are indicated with #.

different spatial scales. A stand is defined as the primary forest mapping and description unit. It consists of relatively homogeneous forest in terms of tree cover and site conditions; however, stand boundaries can also be defined by technical obstacles (rivers, steeps etc.). The stand as a unit ranges from 0.5 to 20 ha, and forest parameters can be collected using either objective or subjective methods. Objective methods are based on randomly distributed sample plots or relascope plots; subjective methods instead use nonrandomly distributed plots or visual estimates.

The ground truth data available for Kättböle consisted of forest stand boundary maps in digital form and field measurements of several forest parameters, including tree height, diameter, and species. The inventory was conducted in 1995 using squared clusters of four sample plots with radius of 10 m, located at corners of each square with a side of 50 m. The clusters were placed in a randomly positioned, systematic grid with a 200-m spacing. Additionally, some measurements of randomly distributed plots were performed in 1996 as a complement. Ground data were therefore collected using an objective and unbiased method. The plot centers were located by differential GPS measurements with a nominal accuracy of approximately 5 m. For each plot, tree height and stem volume were computed and aggregated to the stand level.

In 18 stands, the area-fill factor was measured. This parameter represents the fraction of ground covered by tree crowns from the radar's perspective. To calculate the area-fill factor at 23° (ERS incidence angle), photographs were taken looking vertically upwards through the forest canopy (at least 15 random points for each stand). By thresholding the pictures, it was possible to estimate the area of sky at an incidence angle of $23^\circ (\pm 5^\circ)$ and, hence, the area-fill factor.

In the large area, a sample of plots from the Swedish National Forest Inventory (NFI) was available. The NFI statistical design is based on systematic cluster sampling, using plots arranged in tracts. Each tract is a square having a side length from 300 to 1800 m. Tracts are uniformly distributed over Sweden, their density being higher in the

Southern regions. They are defined as permanent or temporary, depending on whether they will be revisited or not. For each permanent tract, there are eight plots (four in the Southwest region) located on the perimeter, with a radius of 10 m; temporary tracts consist of 12 plots (eight in the Southwest region) with a radius of 7 m (Ranneby, Cruse, Hägglund, Jonasson, & Swärd, 1987). The position of the plots is determined from differential GPS with a nominal accuracy of about 5 m. The original NFI data set consisted of 1004 plots measured between 1994 and 1998. Estimated stem volume was adjusted to the year of satellite imagery using the growth models in Söderberg (1986). From the original set, we removed plots that, even partially, included a land class different than forest. Plots located on non-productive forest land (i.e. having a growth rate $< 1 \text{ m}^3/\text{ha}$ per year) were removed as well. Consequently, the data set was reduced to 723 plots, with stem volume ranging up to $683 \text{ m}^3/\text{ha}$, a mean value of $165 \text{ m}^3/\text{ha}$ and a standard deviation of $124 \text{ m}^3/\text{ha}$.

To aid interpretation, weather statistics including temperature, rain and snow precipitation, wind speed, and wind direction measured periodically during the day were obtained. Data were available from two weather stations 2 and 40 km from the Kättböle site, and from seven stations operated by the Swedish Meteorological and Hydrological Institute (SMHI) located all around the large area. Snow depth measurements were taken in Ultuna and in Kjetslinge, 35 km southeast and 45 km northeast of Kättböle, respectively, and at four SMHI stations (Fig. 1).

2.3. Imagery

For this study, we used imagery acquired by the C-band SARs mounted on the ERS-1 and ERS-2 satellites. Both satellites fly in a sun-synchronous orbit at a height of 785 km, with a repeat-pass cycle of 35 days. However, since the two satellites fly over the same area with a temporal separation of 1 day, the interval between two acquisitions of the same scene becomes as short as 1 day (ERS-1/2

Table 1
Image dates and normal components of the baseline (B_n)

Image dates	B_n [m]
11th/12th June 1995	86
16th/17th July 1995	16
20th/21st August 1995	75
24th/25th September 1995	219
29th/30th October 1995	18
12th/13th March 1996	218
17th/18th March 1996	66
16th/17th April 1996	74
21st/22nd April 1996	55

“tandem” mode). The “tandem” mode lasted from June 1995, when ERS-2 started acquiring, until March 2000, when ERS-1 was finally switched off. The radar antenna, identical on the two satellites, is VV polarised, has a nominal incidence angle of 23° , and covers a swath 100 km wide. The SAR has a 4-m resolution in the along-track direction and an 8-m resolution in the slant-range direction (corresponding to 20 m in the ground-range direction). However, because of speckle, the resolution decreases in both directions.

From the ERS-1/2 “tandem” mode, a set of 18 images was available, corresponding to nine pairs with a 1-day interval between image acquisition. The imagery spans a period of 10 months during 1995 and 1996, covering several meteorological conditions typical of northern latitudes. Table 1 includes a complete listing of acquisition dates and normal components of the baseline. Table 2 reports a summary of the weather conditions at the time of acquisition; according to the data, weather was rather uniform all over the large area.

For each pair, the interferogram was computed; in particular, we considered the coherence images. Since densely forested areas show low coherence, each InSAR processing step in the coherence estimation chain needs to be carefully performed. Following the procedure presented in Santoro, Askne, Smith, Dammert, and Fransson (2000),

before estimation, each pair of images was coregistered at subpixel level, azimuth spectrum filtered (Schwäbisch & Geudtner, 1995), and range wavenumber shift filtered (Gatelli et al., 1994). Coherence was computed by means of the Maximum Likelihood (ML) estimator as follows:

$$\gamma = \frac{\left| \sum_{i=1}^N g_{1,i} g_{2,i} e^{-j\varphi_i} \right|}{\sqrt{\sum_{i=1}^N |g_{1,i}|^2 \sum_{i=1}^N |g_{2,i}|^2}} \quad (1)$$

where $g_{1,i}$ and $g_{2,i}$ denote pixel no. i in the first and second amplitude SAR image, respectively, and $e^{-j\varphi_i}$ is a topography correction factor in which φ_i is obtained from the differential phase image between the two complex SAR images. The window size was set to 5×25 (in range and in azimuth, respectively), equal to 125 samples, N , as it seemed to be a good trade-off between the need for accurate coherence estimation and the spatial resolution of coherence imagery (approximately 100×100 m). Gaussian window functions were used in order to avoid rectangular artifacts due to strong scatterers in the coherence image. The bias for zero coherence, computed over water areas, was found to be 0.135; from this value, the independent number of samples was computed and bias reduction performed (Dammert, 1999b).

A digital elevation model produced by the Swedish National Land Survey, having a pixel size of 50×50 m and a maximum standard error of 2.5 m, was available. For InSAR processing and geocoding of the imagery, the DEM was resampled to smaller pixel sizes using linear interpolation. Over the Kättböle site, a 12.5×12.5 m version was used. For the large area a 25×25 m pixel size was chosen as it represented a good trade-off between resolution and dimension of an image. Thematic maps at a scale of 1:50 000 in digital format, produced by the Swedish National Land Survey between 1994 and 1999, with a geometric accuracy of the order of 10–15 m, were used as a reference to identify landcovers in the large area. These

Table 2
Weather history at date of image acquisition

Image dates	Weather conditions
11th/12th June 1995	Rainfall between passes; $T \cong 10^\circ \text{C}$; wind < 5 m/s
16th/17th July 1995	Rainfall between passes; $T \cong 15^\circ \text{C}$; wind < 4 m/s
20th/21st August 1995	No precipitation; $T \cong 15^\circ \text{C}$; wind < 3 m/s
24th/25th September 1995	Some rain at ERS-2 pass; $T \cong 10^\circ \text{C}$; wind < 4 m/s
29th/30th October 1995	Rainfalls before first pass; $T \cong 0^\circ \text{C}$; wind < 2 m/s
12th/13th March 1996	No precipitation; snow depth $\cong 10$ cm; $T \cong -5^\circ \text{C}$ (just above 0°C between passes); wind < 5 m/s
17th/18th March 1996	Snowfall before first pass; snow depth $\cong 10$ cm; $T \cong -2^\circ \text{C}$ (just below the freezing point between acquisitions); wind < 2 m/s
16th/17th April 1996	No precipitation; no snow; $T \cong 8^\circ \text{C}$ ($> 0^\circ \text{C}$ between passes; $\leq 0^\circ \text{C}$ before first pass); wind < 4 m/s
21st/22nd April 1996	Some precipitation registered between passes (not all stations); $T \cong 13^\circ \text{C}$; wind < 4 m/s

Precipitation, snow depth (if measured), temperature, and wind speed are reported based on data from nine weather stations.

consisted of open land, cultivable land, forested areas, clear-cuts, marshes, urban areas, and water bodies. For our purposes, the digital maps were resampled to a pixel size of 25×25 m.

Using the digital forest stand map in Kättböle, forest stands were localised in the 12.5×12.5 m SAR and InSAR images. In order to reduce border effects on intensity and coherence measurements, the stands were decreased in size by removing a 25-m-wide zone along the perimeter of each stand. To reduce noise in coherence measurements, only stands larger than 2 ha after shrinking were considered. This procedure ensured that all stands included a statistically sufficient number of sample plots to estimate stem volume from field data. Since stands with very low stem volumes, i.e. < 5 m³/ha, look more like an open field rather than a forest, they were not considered. In total, 42 stands were taken into account for analysis, with an area ranging between 2 and 14 ha. Stem volume was distributed between 8 and 335 m³/ha, with average volume of 135 m³/ha, standard deviation of 76 m³/ha and a standard error of about 18%. For each stand, mean backscatter and coherence values were determined from the corresponding images.

The area common to the available SAR imagery and DEM determined the large area analysed in this work. It covered 4235 km² (the maximum distances being 87 and 61 km in the East–West and in North–South directions, respectively). According to the thematic maps, forests and clear-cuts represented 55% and 4% of the investigated area (corresponding to 2348 and 176 km²), respectively. Cultivated land was the main nonforested landcover (29%); lakes, open land, and urban settlements of medium and small sizes represented the remaining landcover classes (12%).

Of the 723 NFI plots previously described in the ground truth data subsection, the large area included 268 plots. Stem volume ranged between 0 and 587 m³/ha, with a mean value of 164 m³/ha and a standard deviation of 124 m³/ha. Since the plot size was smaller than the pixel size in

the 25×25 m images, the coherence value for each plot was taken to be that of the corresponding pixel. However, the number of plots used in this study was decreased to 166 for the following two reasons.

- Since coherence is computed using a window, coherence values of pixels near edges between different landcovers suffer from border effects and, therefore, such measurements are not representative of the landcover in which they belong to. Having used a coherence estimation window of 100×100 m, plots less than two pixels (i.e. 50 m) away from forest edges were removed (83 plots).

- In order to have comparable data sets from Kättböle and the large area, plots with stem volume below 5 m³/ha or above the 350 m³/ha were removed (7 and 12 plots, respectively).

After this operation, the data set included plots with stem volume between 5 and 346 m³/ha, with a stem volume mean value of 164 m³/ha and a standard deviation of 94 m³/ha.

To investigate the potential of stem volume retrieval on a pixel basis, the surveyed sample plots in Kättböle were also considered. The same selection criteria used for the NFI plots were adopted, resulting in a set of 216 plots to be used for further analysis. This data set included plots with stem volume between 6 and 332 m³/ha; the mean value for stem volume was 144 m³/ha and the standard deviation was 81 m³/ha. For both test sites, a summary of the most relevant characteristics is reported in Table 3.

3. Methodology

3.1. Modelling

The short wavelength of the C-band (5.7 cm) is such that, in forested areas, the backscatter can be considered as the sum of two main contributions; one is scattering from the upper part of the forest canopy, the other comes from the ground. The high attenuation of the wave in the first layers of the canopy has the effect that the tree–ground or ground–tree double bounce and backscatter from branches

Table 3
Summary of the most significant ground truth data for the investigated test sites

	Kättböle site	Large area
Area	550 ha	4235 km ² (of which 2348 km ² are forests and 176 km ² clear-cuts).
Ground truth stand level	42 stands Area between 2 and 14 ha Stem volume: 8–335 m ³ /ha Average: 135 m ³ /ha Standard deviation: 76 m ³ /ha Standard error: ca. 18%	
Ground truth plot level	216 plots Area ≤ 314 m ² Stem volume: 6–332 m ³ /ha Average: 144 m ³ /ha Standard deviation: 81 m ³ /ha	166 NFI plots Area ≤ 314 m ² Stem volume: 5–346 m ³ /ha Average: 164 m ³ /ha Standard deviation: 94 m ³ /ha

can be neglected. Starting from these assumptions, in a manner similar to the Water Cloud Model for vegetation (Attema & Ulaby, 1978), we consider a simple model based on radiative transfer through a horizontal scattering and attenuating layer (Askne et al., 1995):

$$\sigma_{\text{for}}^{\circ} = (1 - \eta)\sigma_{\text{gr}}^{\circ} + \eta[\sigma_{\text{gr}}^{\circ}T_{\text{tree}} + \sigma_{\text{veg}}^{\circ}(1 - T_{\text{tree}})] \quad (2)$$

The forest backscatter, $\sigma_{\text{for}}^{\circ}$, is expressed as a function of three contributions due to the ground and to the vegetation. In Eq. (2), each term is weighted by the area-fill factor, η , in order to consider the fraction of ground covered by tree crowns. The first term in Eq. (2) is related to the scattering from the ground through the gaps in the canopy, illustrating that the forest is not a continuous layer. The other two terms are related to the effect of the vegetation and include the backscatter from the ground attenuated by the trees and the backscatter directly from the vegetation, respectively. In Eq. (2), $\sigma_{\text{gr}}^{\circ}$ and $\sigma_{\text{veg}}^{\circ}$ represent the backscatter from the ground and the vegetation layers, respectively, while T_{tree} represents the two-way transmissivity through the tree. This term expresses how much the incoming energy gets attenuated when it passes through the tree canopy. The two-way tree transmissivity factor can be expressed as an exponential, $e^{-\alpha h}$, where α is the two-way attenuation per meter through the tree (in Np/m) and h is the attenuating layer thickness, which we assume to be the same as the tree height.

The expression in Eq. (2) can be rearranged in order to highlight the total scattering from the ground and the scattering due to the vegetation:

$$\sigma_{\text{for}}^{\circ} = \sigma_{\text{gr}}^{\circ}T_{\text{for}} + \sigma_{\text{veg}}^{\circ}(1 - T_{\text{for}}) \quad (3)$$

where

$$T_{\text{for}} = [(1 - \eta) + \eta e^{-\alpha h}] \approx (1 - \eta) \quad (4)$$

represents the two-way transmissivity through the whole forest canopy. Due to the high attenuation in the first few meters of the tree canopy, the two-way tree transmissivity is often almost negligible (Askne, Dammert, & Smith, 1999). Hence, the forest transmissivity can be seen as a simple function of the area-fill factor, as shown in the last term in Eq. (4).

Using measurements by a helicopter borne scatterometer, Pulliainen et al. (1994) has found that the forest transmissivity can be expressed as $e^{-\beta V}$, where V is the stem volume and β is an empirically defined coefficient. Hence, Eq. (3) can be written as:

$$\sigma_{\text{for}}^{\circ} = \sigma_{\text{gr}}^{\circ}e^{-\beta V} + \sigma_{\text{veg}}^{\circ}(1 - e^{-\beta V}) \quad (5)$$

thus relating the total forest backscatter to stem volume. Moreover, considering Eq. (4), from the forest transmissivity definitions, we can write:

$$e^{-\beta V} = 1 - \eta(1 - e^{-\alpha h}) \quad (6)$$

linking two parameters that can be measured (η and α) to an empirical one, β .

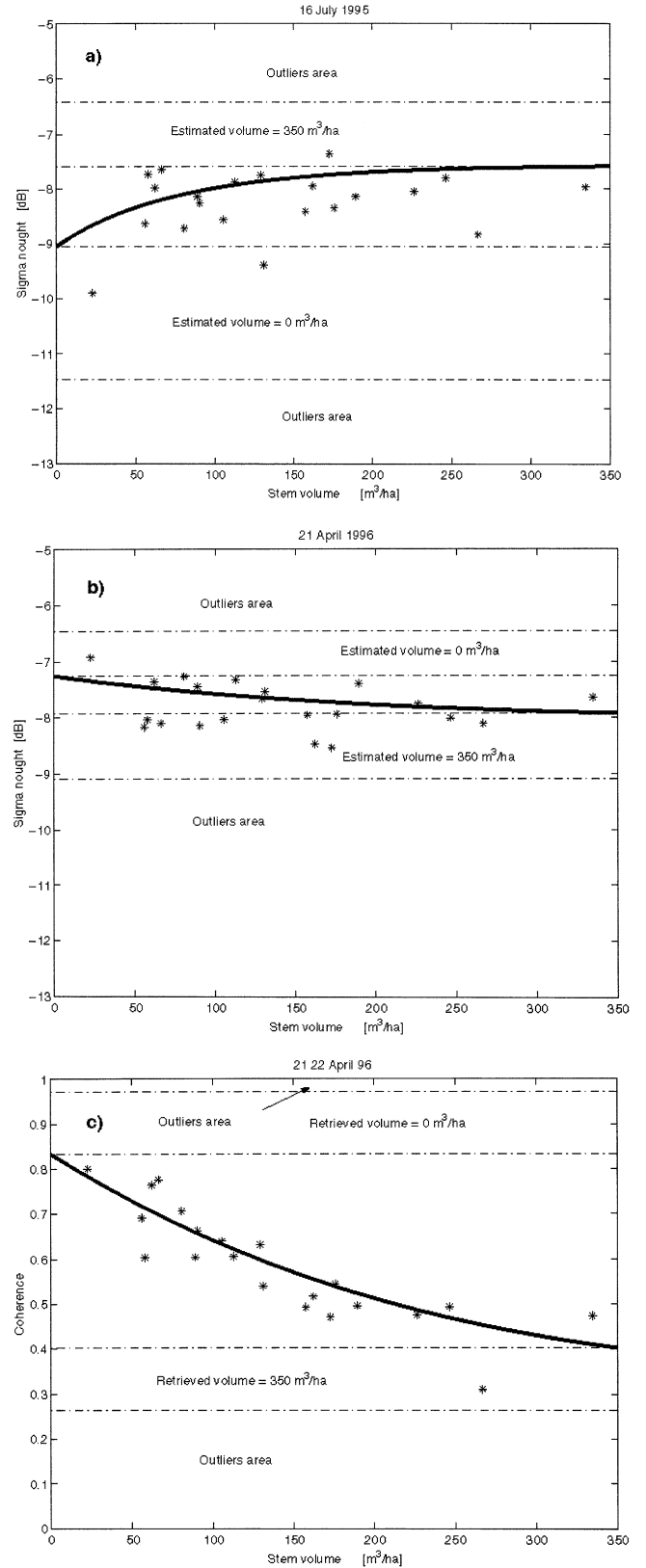


Fig. 2. Stem volume retrieval possibilities as a function of backscatter and coherence. In (a) and (b), the solid line represents the model line from Eq. (5); in (c), the solid line represents the model line from Eq. (9). The outliers area is defined at a distance of two standard deviations from the extreme model values.

Studies on the relationship between backscatter coefficient and stem volume at the C-band have shown saturation of the backscatter already at low stem volumes (about 50–100 m³/ha). Above this level, the backscatter does not provide any relevant information about stem volume. Coherence, instead, does not seem to suffer from the same problem, as pointed out in Askne, Dammert, and Smith (1997). Therefore, this quantity looks more suitable for stem volume retrieval.

$$\gamma = \left| (1 - \eta) \gamma_{\text{gr}} \frac{\sigma_{\text{gr}}^{\circ}}{\sigma_{\text{for}}^{\circ}} + \eta \left[\gamma_{\text{gr}} \frac{\sigma_{\text{gr}}^{\circ}}{\sigma_{\text{for}}^{\circ}} T_{\text{tree}} + \gamma_{\text{veg}} \frac{\sigma_{\text{veg}}^{\circ}}{\sigma_{\text{for}}^{\circ}} \left(\frac{\alpha}{\alpha - j \frac{4\pi B_n}{\lambda R \sin \theta}} \right) \left(e^{-j \frac{4\pi B_n}{\lambda R \sin \theta} h} - T_{\text{tree}} \right) \right] \right| \quad (7)$$

The first two terms in Eq. (7) represent the contribution due to the ground. The temporal coherence of the ground, γ_{gr} , is weighted by the ground backscatter component. The third term in Eq. (7) represents the contribution due to the vegetation. The temporal coherence of the vegetation, γ_{veg} , is weighted by the vegetation backscatter component. The remaining part of this term takes into account the effect of the InSAR system geometry due to a scattering layer with attenuation α and height h (Askne, Dammert, Ulander, et al., 1997). By analogy to topographic phase, the complex exponential in Eq. (7) includes the InSAR system geometry on the total forest coherence, where B_n represents the normal component of the baseline, R the slant range, λ the radar wavelength, and θ the local incidence angle.

Due to the high tree attenuation per meter, the two-way tree transmissivity T_{tree} becomes negligible. Hence, using Eq. (4), we can rewrite Eq. (7) in a simpler way:

$$\gamma = \left| \gamma_{\text{gr}} \frac{\sigma_{\text{gr}}^{\circ}}{\sigma_{\text{for}}^{\circ}} T_{\text{for}} + (1 - T_{\text{for}}) \gamma_{\text{veg}} \frac{\sigma_{\text{veg}}^{\circ}}{\sigma_{\text{for}}^{\circ}} e^{-j \frac{4\pi B_n}{\lambda R \sin \theta} (h - \alpha^{-1})} \right| \quad (8)$$

$$\gamma = \left| \gamma_{\text{gr}} \frac{\sigma_{\text{gr}}^{\circ}}{\sigma_{\text{for}}^{\circ}} e^{-\beta V} + \left(\frac{1 - e^{-\beta V}}{1 - T_{\text{tree}}} \right) \gamma_{\text{veg}} \frac{\sigma_{\text{veg}}^{\circ}}{\sigma_{\text{for}}^{\circ}} \left(\frac{\alpha}{\alpha - j \frac{4\pi B_n}{\lambda R \sin \theta}} \right) \left(e^{-j \frac{4\pi B_n}{\lambda R \sin \theta} h} - T_{\text{tree}} \right) \right| \quad (9)$$

The vegetation backscatter and coherence were assumed to be independent of stem volume, as well as the two-way attenuation per meter, α . The attenuation of the radar signal in mature forest tree canopies is very high; in particular, the value of α was chosen to be 2 dB/m, as suggested in Dammert (1999a). The relation between height and stem volume for the type of forest studied has been modelled according to the following expression (Eq. (10)):

$$h = (aV)^b \quad (10)$$

The coefficients have been estimated from in situ data by means of a least squares regression analysis ($a=2.44$, $b=0.46$). The same relationship has been used in other areas (Askne, Dammert, Ulander, et al., 1997; Santoro et al., 1999) and almost identical values for the coefficients were obtained.

In Eqs. (5) and (9), the backscatter and coherence coefficients for ground and vegetation ($\sigma_{\text{gr}}^{\circ}$, $\sigma_{\text{veg}}^{\circ}$, γ_{gr} , γ_{veg}) are

The relationship between coherence and stem volume has been modelled according to the IWCM described in Askne et al. (1995, 1999), Askne, Dammert, Ulander, and Smith (1997), and Askne and Smith (1996) and fully reviewed in Dammert (1999a). Similar to the idea of the Water Cloud Model, the IWCM considers the total forest coherence as a sum of contributions due to the ground and to the vegetation:

If the normal component of the baseline goes to zero, the forest coherence is determined by the coherence of the individual components weighted by their backscatter and the forest transmissivity, i.e. the area-fill factor. When $B_n \neq 0$, the complex exponential introduces a phase term related to height of the scattering center of the vegetation, $(h - \alpha^{-1})$, i.e. the height of the forest, h , minus the penetration depth, α^{-1} . The model in Eq. (8) reduces to the empirical model presented in Koskinen et al. (2001) if it is assumed that $B_n=0$.

3.2. Regression procedure

Since this study investigated the retrieval of stem volume from coherence data, the area-fill factor in Eq. (7) was expressed as a function of stem volume so that the total forest coherence in Eq. (7) can be written as:

unknown, as well as the two-way forest transmissivity coefficient, β . In this study, a training procedure based on two least squares minimisations between measured backscatter and modelled backscatter from Eq. (5) and between measured coherence and modelled coherence from Eq. (9) was used to estimate the five unknown parameters:

$$\sum_{i=1}^N [\sigma_{\text{meas},i}^{\circ} - \sigma_i^{\circ}(\sigma_{\text{gr}}^{\circ}, \sigma_{\text{veg}}^{\circ}, \beta)]^2 = \min \quad (11)$$

$$\sum_{i=1}^N [\gamma_{\text{meas},i} - \gamma_i(\gamma_{\text{gr}}, \gamma_{\text{veg}}, \beta, \sigma_{\text{gr}}^{\circ}, \sigma_{\text{veg}}^{\circ})]^2 = \min \quad (12)$$

where N represents the number of elements in the training set; $\sigma_{\text{meas},i}^{\circ}$ and $\gamma_{\text{meas},i}$ are the measured backscatter and coherence for the element no. i , while σ_i° and γ_i are the corresponding modelled values according to Eqs. (5) and (9), respectively.

Table 4
Parameter values for regression lines obtained using Eqs. (5) and (9) on the training set data of 21 forest stands from Kättböle

Image dates	γ_{gr}	γ_{veg}	β [ha/m ³]	σ_{gr}^o [dB]	σ_{veg}^o [dB]
11th/12th	0.23	0.10	0.0097	-7.6	-7.2
June 1995	0.23	0.10	0.0108	-8.5	-8.8
16th/17th	0.22	0.09	0.0115	-9.0	-8.3
July 1995	0.22	0.09	0.0131	-7.6	-7.6
20th/21st	0.77	0.36	0.0079	-9.6	-7.7
August 1995	0.77	0.36	0.0074	-10.3	-8.2
24th/25th	0.44	0.21	0.0068	-9.0	-8.1
September 1995	0.44	0.21	0.0071	-9.4	-8.7
29th/30th	0.74	0.58	0.0085	-8.3	-8.6
October 1995	0.74	0.58	0.0092	-8.6	-9.3
12th/13th	0.76	0.18	0.0035	-8.5	-9.3
March 1996	0.77	0.19	0.0034	-9.0	-9.5
17th/18th	0.75	0.21	0.0088	-8.6	-9.3
March 1996	0.75	0.21	0.0089	-9.2	-9.8
16th/17th	0.81	0.54	0.0056	-7.7	-8.2
April 1996	0.81	0.54	0.0059	-7.7	-8.5
21st/22nd	0.83	0.35	0.0056	-7.3	-8.0
April 1996	0.83	0.30	0.0042	-8.1	-8.0

For each pair, the values in the upper row and the lower row have been determined using backscatter data from ERS-1 and ERS-2, respectively.

The training was performed in both cases at the stand level in order to minimise the effect of noise in the backscatter and the coherence measurements. When the procedure was applied in Kättböle, the stands were sorted by stem volume and every second stand included in the training set. The reason for this operation was the limited number of stands available; we needed to split these into a test and a training set, and we still wanted to represent uniformly the range of stem volume in both sets. For the large area, the training set consisted of all the stands in Kättböle in order to have a model fit as

accurate as possible to be then used for the retrieval at the pixel level.

Fitting a line to the backscatter measurements by means of Eq. (11) gave ambiguous results for most of the backscatter images. It was possible to fit a line, but the minimum was often achieved when σ_{veg}^o and β had physically meaningless values. Moreover, we noticed that we would still have achieved a fit close to the one based on Eq. (11) by combining different and more physically significant values of σ_{gr}^o , σ_{veg}^o , and β . The reason for such behaviour should be seen in the large spread of the measurements, which made it almost impossible to define accurate values for the parameters in Eq. (5). Coherence measurements were, in many cases, not affected by spread of values; therefore, we considered them more reliable for training the models. Hence, the estimation of the five parameters was performed as follows:

- Initial computation of ground and vegetation coherence (γ_{gr} and γ_{veg}) and β using Eq. (12), assuming a constant backscatter with respect to stem volume (i.e. $\sigma_{for}^o = \sigma_{gr}^o = \sigma_{veg}^o$). Such assumption reflected indeed the behaviour of backscatter measurements.
- Estimation of σ_{gr}^o and σ_{veg}^o values from Eq. (11), using β computed in the previous step.
- Computation of new values for γ_{gr} , γ_{veg} , and β from Eq. (12), using σ_{gr}^o and σ_{veg}^o obtained in step B.

Steps B and C were iterated until the five parameters did not show any change in their values. Generally, two iterations were sufficient to determine values of all the parameters.

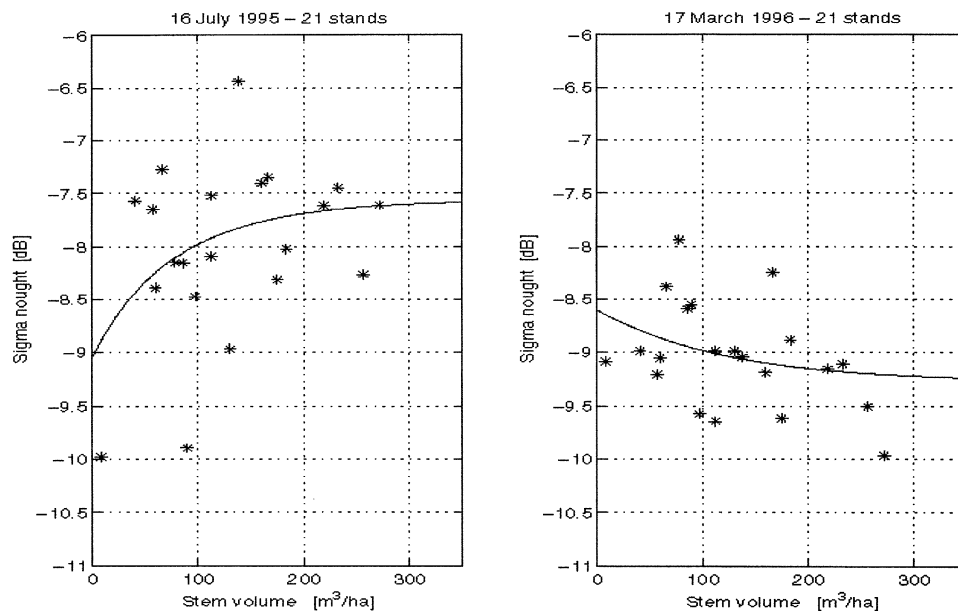


Fig. 3. Regression to backscatter measurements using Eq. (5) for the training set of 21 stands in Kättböle. The two examples show the large spread in the measurements and the saturation at low stem volume.

3.3. Stem volume retrieval from a single image

Once the five parameters have been estimated using the InSAR measurements in the training set, it is possible to retrieve stem volume for an independent set of stands (test set) with a numerical inversion of Eqs. (5) and (9). For the Kättböle site, the remaining stands were used as a test set, and retrieval was performed both at the stand and plot levels. For the large area, all forested pixels according to the digital maps were included in the test set, the NFI plots described in the previous section being a part of it.

In some cases, the inversion could not be performed because the measurements were either too high or too low, resulting in unrealistic stem volume estimates, i.e. below zero or much higher than is typical for the region. When this occurred, some assumptions were considered in order to associate a stem volume to every sample (see Fig. 2).

For the backscatter, we may encounter two situations. When $\sigma_{gr}^0 < \sigma_{veg}^0$, the model line from Eq. (5) increases with stem volume. Samples with backscatter above the maximum model value were given a stem volume of $350 \text{ m}^3/\text{ha}$; those with backscatter below the minimum model value were given a stem volume of $0 \text{ m}^3/\text{ha}$. When $\sigma_{gr}^0 > \sigma_{veg}^0$, the model line from Eq. (5) decreases with stem volume. Samples with backscatter above the maximum model value were given a stem volume of $0 \text{ m}^3/\text{ha}$; those with backscatter below the minimum model value were given a stem volume of $350 \text{ m}^3/\text{ha}$. For coherence, we assumed that a test sample had stem volume equal to $0 \text{ m}^3/\text{ha}$ when it had coherence above the maximum value in Eq. (9) or $350 \text{ m}^3/\text{ha}$ when it was below the minimum value in Eq. (9). However, when a sample was at least two standard deviations above the maximum level or below the minimum level in Eq. (9), it was considered an outlier, and no value was retrieved for it.

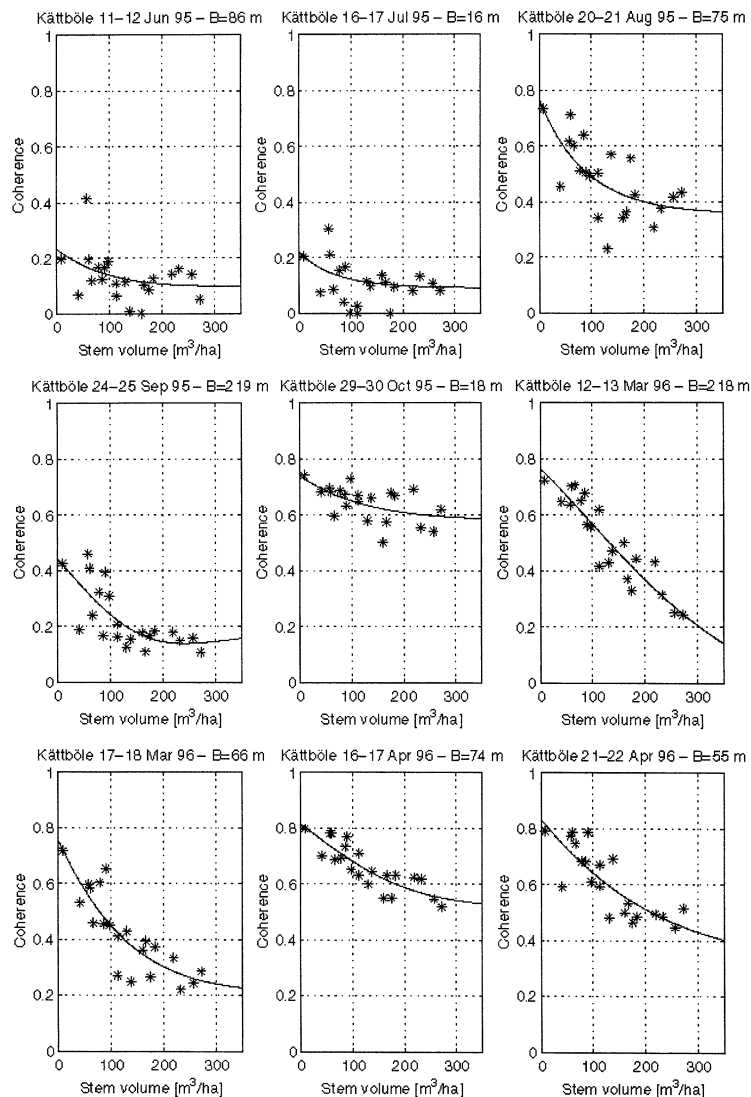


Fig. 4. Regression lines obtained using Eq. (9) for the training set of 21 stands in Kättböle. Points at zero coherence are a result of bias reduction.

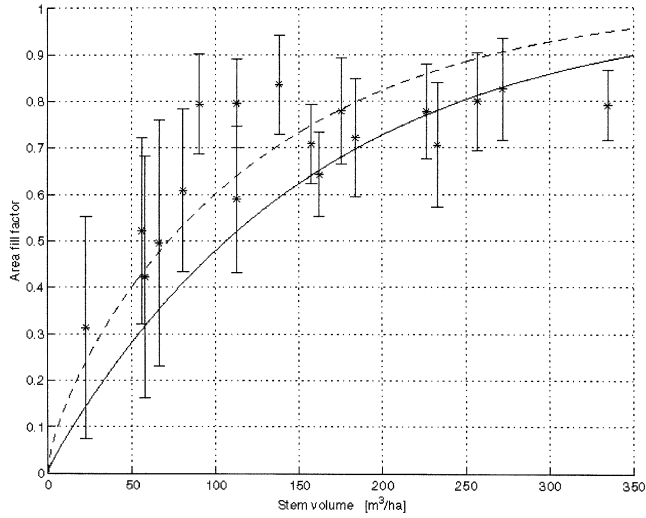


Fig. 5. Area-fill factor at stand level and regression analysis. The vertical bars express the variability of area-fill factor measurements in a stand; in particular, they represent one standard deviation from the mean value. The dashed line represent a least squares regression to area-fill factor measurements using Eq. (6) (results: $\alpha=0.62$ dB/m and $\beta=0.0069$ ha/m³). The solid line represents the area-fill factor computed from Eq. (6) using $\alpha=2$ dB/m and $\beta=0.0065$ ha/m³.

To describe the results of the retrieval the following statistical parameters were calculated the following.

(a) The root mean square error (RMSE):

$$\text{RMSE} = \sqrt{\frac{1}{N_{\text{test}}} \sum_{i=1}^{N_{\text{test}}} (V_i - V_i^{\text{gt}})^2 - 0.5 \frac{1}{N_{\text{test}}} \sum_{i=1}^{N_{\text{test}}} (\text{S.E.}_i)^2} \quad (13)$$

In Eq. (13), N_{test} is the number of samples in the test set, V_i and V_i^{gt} are the retrieved stem volume and the stem volume estimated from the ground truth for sample no. i . The second term takes into account sampling errors in the ground truth at the stand level, where S.E. _{i} represents the standard error for stand no. i , and the factor 0.5 is a correction due to systematic sampling design, in accordance with the empirical investigation by Lindgren (1984).

(b) The squared coefficient of correlation, R^2 .

3.4. Multitemporal retrieval

Stem volume estimates from single coherence and backscatter images can be combined in order to determine a so-called “multitemporal” estimate. For each element in the test set, a linear combination of stem volume estimates was used according to:

$$V_{\text{multitemp},j} = \sum_{i=1}^M w_i V_{i,j} \quad (14)$$

where $V_{\text{multitemp},j}$ gives the multitemporal retrieved stem volume for the j th element in the test set using stem volume estimates from M images. In Eq. (14), $V_{i,j}$ is the estimated value from image no. i for the j th element in the test set. The weighting coefficients w_i are related to each image used for the multitemporal retrieval and are defined as follows:

$$w_i = \frac{\left(\frac{p_{\text{train},j} p_{\text{test},j}}{\text{RMSE}_j^2} \right)}{\sum_{j=1}^M \left(\frac{p_{\text{train},j} p_{\text{test},j}}{\text{RMSE}_j^2} \right)} \quad (15)$$

The idea behind Eq. (15) is that images with lower residuals, RMSE_j , should have more weight to determine the multitemporal estimate of stem volume. To reduce the effect of images that show a large dispersion of measurements along the modelled line, for each backscatter and coherence image, we considered the percentages of measurements that can be correctly classified (i.e. measurements between the maximum and the minimum modelled value) both in the training and in the test set ($p_{\text{train},i}$ and $p_{\text{test},i}$).

4. Results

4.1. Modelling

Using the models in Eqs. (5) and (9), lines have been fitted to the backscatter and coherence training measurements for each image. The values of the five initially

Table 5
RMSE, corrected for ground truth estimation errors, and R^2 for each single coherence and intensity image at stand level in Kättböle (21 stands)

Image dates	Coherence		ERS-1 backscatter		ERS-2 backscatter	
	RMSE [m ³ /ha]	R^2	RMSE [m ³ /ha]	R^2	RMSE [m ³ /ha]	R^2
11th/12th June 1995	151.5	.04	160.2	.01	191.4	.04
16th/17th July 1995	123.8	.39	118.6	.01	133.7	.06
20th/21st August 1995	88.5	.46	82.4	.19	113.6	.04
24th/25th September 1995	73.6	.37	97.6	.36	139.7	.07
29th/30th October 1995	96.9	.23	198.3	.04	143.6	.01
12th/13th March 1996	20.9	.92	115.8	.16	183.7	.11
17th/18th March 1996	38.4	.74	155.4	.08	155.8	.08
16th/17th April 1996	35.8	.77	167.1	.03	148.9	.01
21st/22nd April 1996	35.6	.74	170.7	.03	163.1	.04

Table 6
RMSE, corrected for the ground truth estimation errors, and R^2 or multitemporal retrieval at stand level in Kättböle (21 stands)

Images combined	RMSE [m^3/ha]	R^2
18 intensity images	74.2	.13
9 coherence images	10.4	.93
All images (27)	10.8	.93
4 coherence images (March and April 96)	10.0	.94

unknown parameters are shown in Table 4. Due to the large spread in the measurements, the backscatter parameters varied greatly and the modelled backscatter turned out to have little significance. Fig. 3 reports two examples, characteristic for the data set available. Coherence turned out to be more significant than backscatter. Fig. 4 shows measured and modelled coherence with respect to stem volume for each InSAR pair.

From Eq. (6), it is possible to relate the area-fill factor, η , to the attenuation, α , and the empirical coefficient β , i.e. $\eta = \eta(\alpha, \beta)$. Using this expression, on the one hand, we performed a least squares regression to the area-fill factor measurements, estimating α equal to 0.62 dB/m and β equal to 0.0069 ha/m^3 . On the other hand, taking the suggested value for α (2 dB/m) and a typical value for β from Table 4 (0.0065 ha/m^3), we computed the area-fill factor as a function of stem volume. Fig. 5 shows the lines for the two cases and the area-fill factor measurements. The different values of α could be explained by performing a sensitivity analysis of the area-fill function to α and β

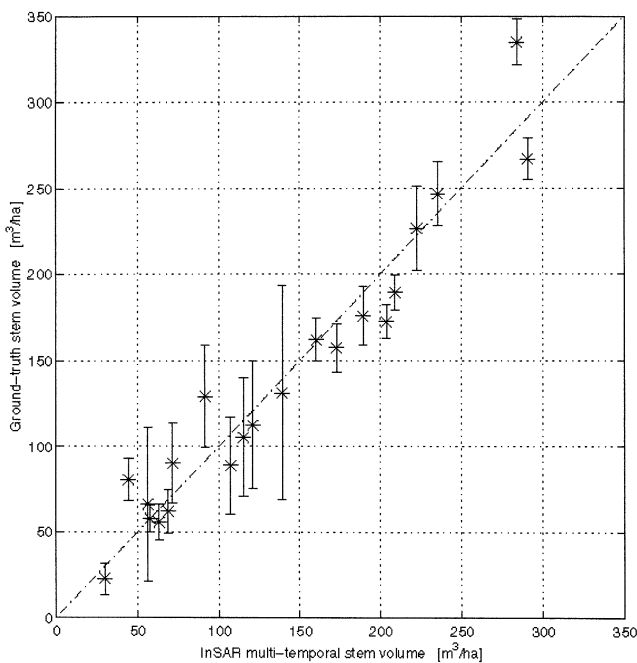


Fig. 6. Comparison between InSAR multitemporal stem volume and stem volume estimated from in situ measurements in Kättböle at stand level (21 stands). The error bars show the standard deviation in the estimated ground truth stem volumes. RMSE=10 m^3/ha (corrected for ground truth errors) and $R^2=.94$.

Table 7
RMSE, without correction for ground truth errors because negligible, and R^2 at plot level in Kättböle (216 test plots)

Image dates	RMSE [m^3/ha]	R^2
12th/13th March 1996	62.9	.50
17th/18th March 1996	80.4	.25
16th/17th April 1996	81.5	.21
21st/22nd April 1996	77.7	.35
Combination of the four images	55.0	.56

Median filtering reduced the error by 5–10 m^3/ha .

separately. The function showed different slopes for small changes of β but seemed to be almost independent of α .

4.2. Stem volume retrieval in Kättböle

For the retrieval in Kättböle, RMSE and R^2 values have been computed both at the stand and at plot levels. At the stand level, the two quantities have been calculated for each coherence and intensity image. Since measurements of ground truth errors for the stands were available, it was possible to correct the retrieval error using the second term in Eq. (13). Tables 5 and 6 report RMSE and R^2 values for the single image and for the multitemporal retrieval, respectively. Fig. 6 shows a comparison between stem volume estimated from in situ measurements and multitemporal estimated stem volume.

At the plot level, retrieval was performed using only the images that performed the best in the stand-wise analysis, i.e. we only considered the four coherence images acquired in March and in April 1996. Since stem volume was retrieved on a pixel basis, geometric mismatch between field and image data and noise in coherence estimation (an important factor in low coherence areas such as forests) could degrade the retrieval accuracy. To mitigate this, the retrieval was

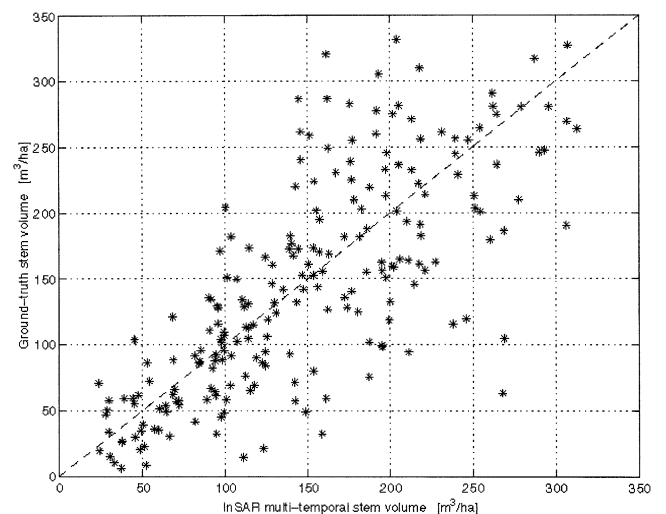


Fig. 7. Comparison between InSAR multitemporal stem volume and in situ values in Kättböle at plot level (216 plots). The original coherence images were median filtered with a 3×3 window. RMSE=55 m^3/ha and $R^2=.56$.

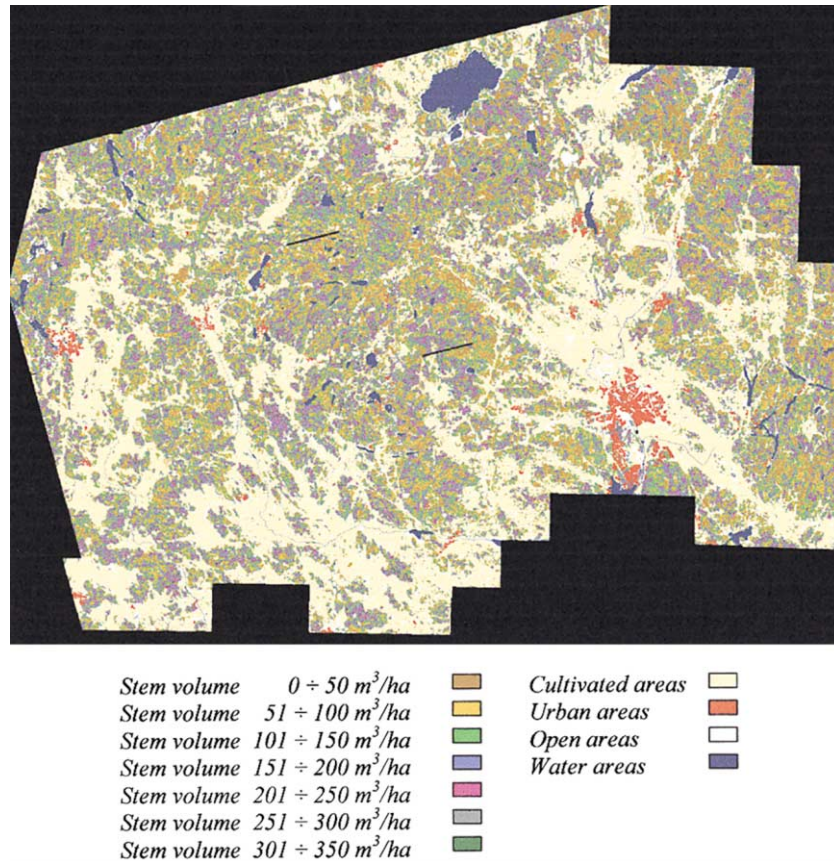


Fig. 8. Forest stem volume map over the large area. The stem volume estimates are superimposed onto the digital landcover map. Pixel size 25 × 25 m. The stem volume has been retrieved for each pixel using a multitemporal combination of four pairs acquired in March and April 1996. For displaying reasons, stem volume values have been grouped in intervals of 50 m³/ha.

performed on median-filtered images. A 3 × 3 window was preferred in order not to decrease the resolution and to take into account the relative shifts between images, which were visually estimated to be up to one pixel, i.e. 25 m. RMSE values were calculated using only the first term in Eq. (13), since errors for the ground truth at the plot level could be assumed to be negligible. The single-pair retrieval resulted in RMSE values between 62.9 and 81.5 m³/ha, and R^2 lower than .50. With the multitemporal approach, the error was 55.0 m³/ha and R^2 was equal to .56 (Table 7). Fig. 7 shows a comparison between stem volume estimated from in situ measurements and multitemporal estimated stem volume.

4.3. Stem volume retrieval in the large area

When the retrieval procedure was applied on the large area, we considered once again only those images that performed the best in Kättböle, i.e. the four coherence images acquired in March and April 1996. For each pair, lines from Eqs. (5) and (9) were fitted to the training set; the five unknown parameters resulted to be very similar to those reported in Table 4. Over all forested areas, retrieval from each pair and in a multitemporal fashion was performed on a pixel basis. Coherence images were median-filtered using a

3 × by 3 window for the same reasons discussed in the previous subsection. The retrieval output is illustrated as a

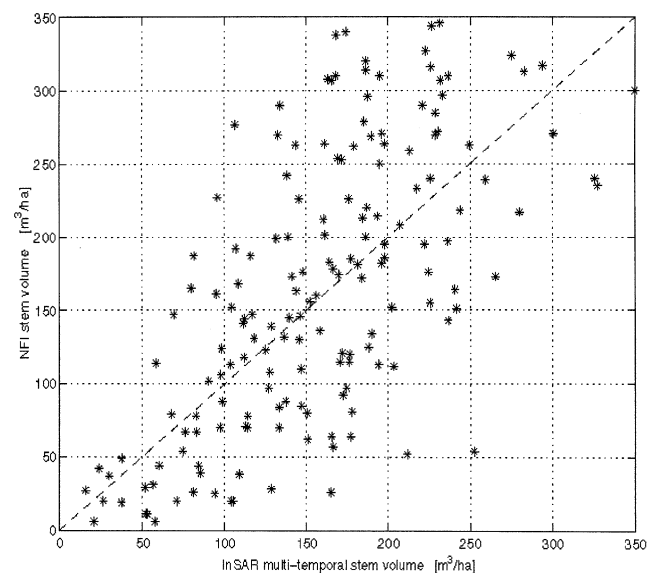


Fig. 9. Comparison between multitemporal and NFI stem volume estimates in the large area at plot level (166 plots). The original coherence images were median filtered with a 3 × 3 window. RMSE = 71.2 m³/ha and R^2 = .43.

Table 8
RMSE, without correction for ground truth errors because negligible, and R^2 coefficient for 166 NFI plots

Image dates	RMSE [m ³ /ha]	R^2
12th/13th March 1996	77.8	.36
17th/18th March 1996	114.3	.12
16th/17th April 1996	111.3	.16
21st/22nd April 1996	100.3	.21
Combination of the four images	71.2	.43

Median filtering reduced the error by 5–10 m³/ha.

stem volume map (Fig. 8), the quality of which could not be verified extensively due to the unavailability of extensive inventoried measurements. Only a comparison between stem volume data from the NFI plots and the estimated values extracted from the maps could be performed.

The single-pair retrieval resulted in RMSE values between 77.8 and 114.3 m³/ha and R^2 lower than .36. With the multitemporal approach, the error was 71.2 m³/ha and R^2 was equal to .43. Once again, the median filtering reduced the error by 5–10 m³/ha. A comparison between retrieved and ground truth stem volume showed some overestimation at low stem volumes and underestimation for denser plots (Fig. 9). In Table 8, retrieval statistics are listed. As for Kättböle plots, the retrieval error was not corrected because the ground truth error at the plot level can be assumed negligible.

5. Discussion

5.1. Modelling

Saturation of backscatter occurred at very low stem volumes in all images; in some cases, the model lines from Eq. (5) were almost horizontal. The large spread of the data and the predominance of stands with stem volume above the saturation level introduced a large uncertainty in the ground and vegetation backscatter coefficients. Even though, σ_{gr}^o , σ_{veg}^o , and β show some changes between acquisitions, the coherence parameters did not seem to be affected. The phase term related to the InSAR geometry in Eq. (9) becomes relevant when the normal component of the baseline is above 200 m. To test the importance of the baseline dependence, a model fit was performed assuming $B_n=0$. Pairs with short baseline showed little difference in the γ_{veg} and β values. The two pairs with $B_n>200$ m showed a negative value for γ_{veg} instead, being therefore physically meaningless, and a very low value of β , thus implying an almost transparent canopy in terms of transmissivity. This illustrates the need to include the effects of the baseline in the forest coherence model.

Table 4 highlights the strong dependence of backscatter and coherence on weather conditions. In June and July, rainfall between passes completely decorrelated the scene and changed the backscatter, even though it is not clear why

this decreased in June. Some rain at ERS-2 acquisition was registered in September, which could explain the relatively low value of γ_{gr} . In two cases (October and 16th/17th April) γ_{veg} was high, and the whole scene showed high coherence. Weather data reported temperatures oscillating around the freezing point and rainfall before the first pass in October and residual frost in April. Pairs with stable weather conditions between passes (August and 21st/22nd April) showed lower values for γ_{veg} . The lowest values were typical of pairs with snow covering the ground and temperature below 0 °C (both March pairs).

The parameter β was constant in most of the cases analysed and in accordance with previous results (Kurvonen et al., 1999; Pulliainen et al., 1994). Values computed for the June and July passes have no physical meaning because of the total decorrelation of the scene. The low value of the 12th/13th March pair might be related to a combined effect of weather and the large baseline. The September pair also had a large baseline but showed a value for β similar to the other pairs.

Fig. 5 shows the relation between the area-fill concept and the transmissivity definition in Eq. (6). In other words, the forest transmissivity could be obtained from measurements of the area-fill factor. Only for the 12th/13th March pair did a disagreement occurred, probably due to the weather and the large baseline.

5.2. Stem volume retrieval

At the stand level, stem volume could be predicted more accurately using coherence rather than intensity; best results were achieved in winter-type pairs, in contradiction with Hyypä and Engdahl (2000). Backscatter data and coherence from pairs with meteorological changes between passes did not provide any information. Compared to single-image retrieval, the multitemporal estimation predicted stem volume more accurately. When images were combined, the retrieval error was lower than the one of each single image included in the combination; nevertheless, the decrease of the RMSE was different depending on which images were combined. The combination of coherence images performed much better than the one based only on intensity images as shown in Table 6. Moreover, adding intensity images to coherence images did not improve the accuracy. The best result was obtained when only winter-type pairs without meteorological changes between acquisitions were considered, reaching an error comparable to the ground truth value. Increasing the number of pairs combined did not reduce the error (Table 6).

Both in Kättböle and in the large area, the retrieval on a plot basis performed better with the multitemporal approach. However, the error was higher than the one obtained at the stand level. Figs. 7 and 9 show that the discrepancy between measured and retrieved stem volume is rather uniform at stem volumes below 200 m³/ha, even though for the large area, there is a tendency towards overestimation. Above 200 m³/ha, the discrepancy increases, leading to under-

estimation for increasing stem volume. Such behaviours can be related to the following two factors.

(1) Errors in plot coordinates and relative shifts between images. This is a factor independent of stem volume range. In vegetated areas, positioning using GPS systems suffers from errors; hence, the coordinates of a plot include a slight inaccuracy. Moreover, the geocoding can introduce an error when an image is transformed to a particular coordinate system. Hence, a plot and the corresponding pixel in the coherence images might not coincide. Consequently, the stem volume of a plot does not always correspond to the retrieved value. The use of a median filter helped in reducing this effect.

(2) Effect due to coherence estimation and lower sensitivity of coherence at high stem volume. The coherence given by Eq. (1) is only an estimate of the true coherence, and at low coherence, i.e. at high stem volumes, the estimates are less accurate, as shown in Askne, Dammert, Ulander, et al. (1997). An error in the estimated coherence implies an error in the retrieved stem volume. Moreover, since at high stem volumes, the slope of coherence estimates can decrease, the retrieval can suffer from larger errors than at small stem volumes.

These factors are stronger at the plot level than at the stand level, where averaging is performed. Averaging reduces the effect of imagery misplacement and the errors in coherence estimation.

At the plot level, a comparison between RMSEs from Kättböle and the large area (Tables 7 and 8) shows that

the accuracy of the multitemporal retrieval from the large area is 29% worse than in Kättböle. This behaviour could be due to the spatial variation of the model parameters, which degrades the performance of stem volume retrieval in large areas.

Table 8 shows big RMSE values in the large area for the 17th/18th March and 16th/17th April. In order to understand what caused such a result, we compared retrieved stem volume from each of the four pairs used for the analysis of the large area. Four squares were therefore randomly placed in the large area. The squares all had the same size, which was randomly chosen in an interval between 1 and 25 km². In this way, we ensured a sufficient number of pixels without introducing too much noise in the analysis. For each area, we plotted the retrieved stem volume values from two pairs against each other, thus obtaining plots like those in Figs. 10 and 11.

The scatterplots for the 12th/13th March and 21st/22nd April (Fig. 10) pairs showed an agreement between retrieved stem volumes up to about 200 m³/ha. Above this level, reduced sensitivity of coherence to stem volume could be noticed. These results confirmed that both pairs were suitable for retrieval in the large area. When we compared one of those pairs with the 17th/18th March pair, we obtained different results depending on where the square was placed (Fig. 11). This behaviour could be explained in terms of different weather effects in the large area. Even though weather data for this pair showed rather similar conditions over the large area, the generally unset-

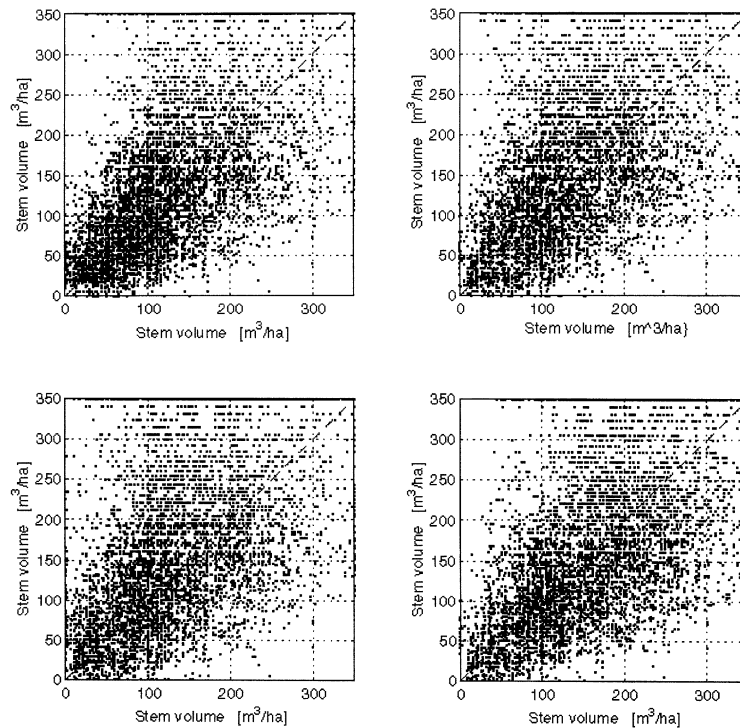


Fig. 10. Scatterplots of retrieved stem volume for the pairs acquired on 12th/13th March (horizontal axis) and 21st/22nd April (vertical axis). The estimates in the subplots were extracted from four squares randomly placed on stem volume maps obtained from each pair. The area of each square was equal to 7.3 km².

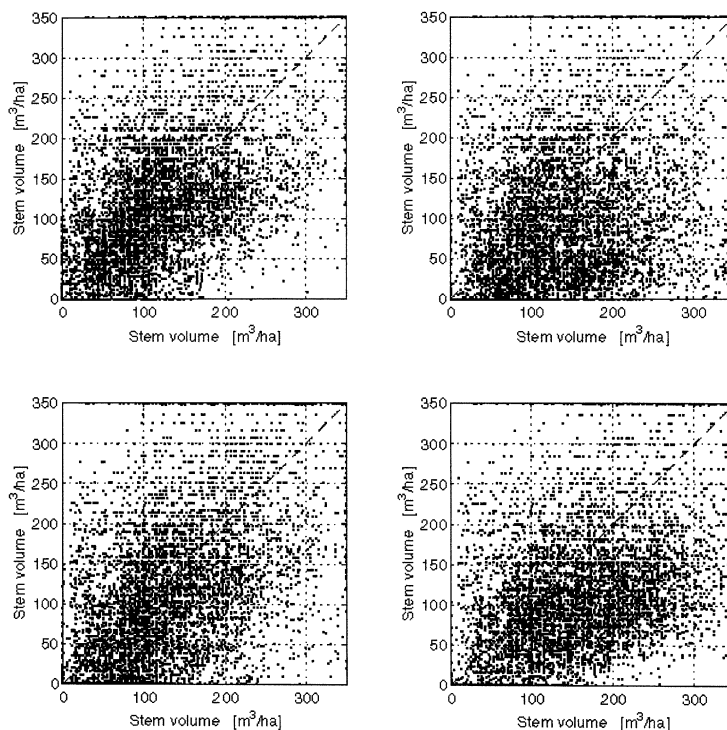


Fig. 11. Scatterplots of retrieved stem volume for the pairs acquired on 12th/13th March (horizontal axis) and 17th/18th March (vertical axis). The estimates in the subplots were extracted from the same four squares randomly placed on stem volume maps described in Fig. 10.

tled weather (snowfall and temperature around freezing) may have resulted in significant local variations. When the comparison was performed with the 16th/17th April pair, the scatterplots looked identical, thus meaning that the effect of weather was identical all over the area. However, for this pair, the scatterplots clearly showed underestimation, which could be related to saturation effects. Even though the pair showed a model line with a rather small slope, we decided to use it for the retrieval in the large area because of the accurate results obtained at the stand level in Kättböle.

In Kättböle and in part of the large area, Fazakas, Nilsson, and Olsson (1999) carried out an analysis using Landsat optical data, making it possible of a comparison. At the plot level, the relative errors, i.e. the ratio of RMSE and mean measured stem volume, show that the retrieval based on InSAR data performed better in both areas. While the relative error was reported to be above 66% using optical data, the multitemporal combination of InSAR based estimates reached a level of 43%. When averaging over larger areas, a value $<10\%$ was achieved for areas as large as 100 ha in Kättböle from optical data, whereas using InSAR data, the accuracy reached a value of 7% at the stand level between 2 and 14 ha. These results show a higher potential of InSAR for stem volume retrieval at the plot level. Moreover, it shows the ability to retrieve stem volume in small averaging units such as stands. However, it should be stressed that this comparison was based on small areas and not completely identical conditions.

6. Conclusions

In this study, we investigated a procedure based on InSAR data for stem volume retrieval in boreal forests at the stand level and on a pixel basis. The relationship of coherence and intensity with respect to stem volume could be described in terms of simple and robust models, which took into account both forest parameters (tree transmissivity, area-fill factor) and InSAR geometry (baseline). The modelling illustrates the importance of the area-fill concept and the normal component of the baseline, B_n . Hence, these two factors should be taken into account for a physically correct InSAR forest model.

Values of the model parameters show how weather conditions affect InSAR data of forested areas. Retrieval of stem volume is characterised by smaller errors when it is based on coherence rather than on intensity. From the analysis, it appears that pairs acquired during the winter perform better, while those when the weather changed between acquisitions do not provide any information and, therefore, should not be considered.

Multitemporal combination of stem volume estimates from single images increases the accuracy of the retrieval. Since intensity images do not provide any additional information to coherence images, the combination of coherence images only is enough. Preferably, pairs acquired during the winter in stable weather conditions should be used. At the stand level, stem volume estimates from the multitemporal approach have been shown to have accuracy comparable

with the ground truth estimates. The availability of accurate in situ measurements is fundamental both for correct training and a correct evaluation of the results. Even though the errors achieved at the pixel level are reasonable, they are not comparable with those achieved at the stand level.

The need to test the retrieval procedure in a relatively large area nearby the Kättböle site, where weather conditions could possibly not influence the accuracy, lead to the production of stem volume maps. The pairs that gave the most accurate results in Kättböle were used for the pixel-based retrieval assuming that they could have worked equally well in the large area. Since extensive in situ forest data were not available, the quality of the stem volume maps could not be fully evaluated. Some information about the retrieval technique in the large area at the pixel level was provided by a set of NFI plots, which confirmed the results found at the Kättböle site. There are several sources of error that have smaller effect at the stand level than at the plot level because of averaging. The spatial variation of the model parameters should also be considered as it might introduce errors in the stem volume retrieval over large areas.

By comparing stem volume estimates in different parts of the large area, it was found that two of the pairs used for the retrieval in the large area were not useful because of different weather effects over the area and saturation of coherence. A comparison between the two remaining pairs showed that for the area investigated, stem volume is estimated consistently up to about 200 m³/ha. For denser forest, discrepancies can occur due to the greater noise in coherence estimates and to the reduced sensitivity of these estimates to stem volume.

To conclude, this study shows that a method based on SAR interferometric data, using the IWCM and a multi-temporal approach, can be used for stem volume retrieval in boreal forests at the stand level up to 350 m³/ha. Retrieval at the plot level seems to be limited because plots are too small compared to the resolution of coherence imagery. Hence, future studies should investigate the retrieval of stem volume in stands distant from a training area, where field data have been accurately measured and weather had the same effects.

Acknowledgments

Dr. Patrik Dammert is acknowledged for his continuous help and advisory, and for the coherence estimation software. Dr. Mats Nilsson, SLU, Umeå, is acknowledged for providing the NFI plot data. We are very thankful to SMHI for providing the weather data in the large area. Snow data measured in Ultuna and Kjettslinge are available at <http://130.28.110.134:80/bgf/verksamh/database.htm>. The interferometric processing of the images was performed with the ISAR toolbox from ESA and with the DIAPASON software from CNES. Funding for the research was

provided from the Swedish National Space Board. All images were provided by the European Space Agency through AOT-S104.

References

- Askne, J., Dammert, P., Fransson, J., Israelsson, H., & Ulander, L. M. H. (1995). Retrieval of forest parameters using intensity and repeat-pass interferometric SAR information. In: *Retrieval of bio- and geophysical parameters from SAR data for land applications* (pp. 119–129). ACTES.
- Askne, J., Dammert, P. B. G., & Smith, G. (1997). Interferometric SAR observations of forested areas. *Third ERS Symposium on Space at the Service of Our Environment* (pp. 337–344). Noordwijk, The Netherlands: ESA Publications Division, ESTEC.
- Askne, J., Dammert, P. B. G., & Smith, G. (1999). Understanding ERS InSAR coherence of boreal forests. In: *IGARSS'99* (pp. 2111–2114). Piscataway, NJ: IEEE.
- Askne, J., Dammert, P. B. G., Ulander, L. M. H., & Smith, G. (1997). C-band repeat-pass interferometric SAR observations of the forest. *IEEE Transactions on Geoscience and Remote Sensing*, 35 (1), 25–35.
- Askne, J., & Smith, G. (1996). Forest INSAR decorrelation and classification properties. In: *Fringe 96 workshop: ERS SAR interferometry* (pp. 95–103). Noordwijk, The Netherlands: ESA Publications Division, ESTEC.
- Attema, E. P. W., & Ulaby, F. T. (1978). Vegetation modeled as a water cloud. *Radio Science*, 13 (2), 357–364.
- Castel, T., Martinez, J.-M., Beaudoin, A., Wegmüller, U., & Strozzi, T. (2000). ERS INSAR data for remote sensing hilly forested areas. *Remote Sensing of Environment*, 73, 73–86.
- Dammert, P. B. G. (1999a). Interferometric Tree Heights—Measurements and Modeling. Research Report 183, Department of Radio and Space Science, Chalmers University of Technology, Gothenburg, Sweden.
- Dammert, P. B. G. (1999b). Spaceborne SAR Interferometry: Theory and Applications. PhD thesis, Technical Report, 382, Department of Radio and Space Science, Chalmers University of Technology, Gothenburg, Sweden.
- Dobson, M. C., Ulaby, F. T., Pierce, L. E., Sharik, T. L., Bergen, K. M., Kellendorfer, J., Kendra, J. R., Li, E., Lin, Y. C., Nashashibi, A., Sarabandi, K., & Siqueira, P. (1995). Estimation of forest biophysical characteristics in Northern Michigan with SIR-C/X-SAR. *IEEE Transactions on Geoscience and Remote Sensing*, 33 (4), 877–895.
- Fazakas, Z., Nilsson, M., & Olsson, H. (1999). Regional forest biomass and wood volume estimation using satellite data and ancillary data. *Agricultural and Forest Meteorology*, 98–99, 417–425.
- Floury, N., Le Toan, L., & Souyris, J. C. (1996). Relating forest parameters to interferometric data. In: *IGARSS'96* (pp. 975–977). Piscataway, NJ: IEEE.
- Fransson, J. E. S., & Israelsson, H. (1999). Estimation of stem volume in boreal forests using ERS-1 C- and JERS-1 L-band SAR data. *International Journal of Remote Sensing*, 20 (1), 123–137.
- Fransson, J. E. S., Smith, G., Askne, J., & Olsson, H. (2001). Stem volume estimation in boreal forests using ERS-1/2 coherence and SPOT XS optical data. *International Journal of Remote Sensing*, 22 (14), 2777–2791.
- Gatelli, F., Guarnieri, A. M., Parizzi, F., Pasquali, P., Prati, C., & Rocca, F. (1994). The wavenumber shift in SAR interferometry. *IEEE Transactions on Geoscience and Remote Sensing*, 32 (4), 855–865.
- Häme, T., Salli, A., & Lahti, K. (1992). Estimation of carbon storage in boreal forests using remote sensing data, M. Kanninen and P. Anttila, pilot study. In: *The Finnish Research Programme on Climate Change, progress report* (pp. 250–255). Helsinki, Finland: Academy of Finland.
- Hyypä, J., & Engdahl, M. (2000). Verification of the capability of repeat-pass SAR interferometry to provide tree height information in boreal forest zone. In: *IGARSS 2000* (pp. 402–404). Piscataway, NJ: IEEE.

- Hyypä, J., Hyypä, H., Inkinen, M., Engdahl, M., Linko, S., & Zhu, Y.-H. (2000). Accuracy comparison of various remote sensing data sources in the retrieval of forest stand attributes. *Forest Ecology and Management*, 128 (1–2), 109–120.
- Koskinen, J. T., Pulliainen, J. T., Hyypä, J. M., Engdahl, M. E., & Hallikainen, M. T. (2001). The seasonal behaviour of interferometric coherence in boreal forest. *IEEE Transactions on Geoscience and Remote Sensing*, 39 (4), 820–829.
- Kurvonen, L., Pulliainen, J., & Hallikainen, M. (1999). Retrieval of biomass in boreal forests from multitemporal ERS-1 and JERS-1 SAR images. *IEEE Transactions on Geoscience and Remote Sensing*, 37 (1), 198–205.
- Lindgren, O. (1984). A study on circular plot sampling of Swedish forest compartments. Report 11, Department of Biometry and Forest Management, Swedish University of Agricultural Sciences, Umeå, Sweden.
- Martinez, J. M., Beaudoin, A., Wegmüller, U., Le Toan, T., & Strozzi, T. (1998). Influence of biophysical, meteorological and topographic factors on multitime ERS tandem data acquired over forested terrain. In: *IGARSS'98* (pp. 1818–1821). Piscataway, NJ: IEEE.
- Pulliaainen, J. T., Heiska, K., Hyypä, J., & Hallikainen, M. T. (1994). Backscattering properties of boreal forests at the C- and X-bands. *IEEE Transactions on Geoscience and Remote Sensing*, 32 (5), 1041–1050.
- Pulliaainen, J. T., Mikkilä, P. J., Hallikainen, M. T., & Ikonen, J.-P. (1996). Seasonal dynamics of C-band backscatter of boreal forests with applications to biomass and soil moisture estimation. *IEEE Transactions on Geoscience and Remote Sensing*, 34 (3), 758–770.
- Ranneby, B., Cruse, T., Häggglund, B., Jonasson, H., Swärd, J., (1987). Designing a new national forest survey for Sweden. *Studia Forestalia Suecica 177*, Faculty of Forestry, Swedish University of Agricultural Sciences, Uppsala, Sweden.
- Santoro, M., Askne, J., Dammert, P. B. G., Fransson, J. E. S., & Smith, G. (1999). Retrieval of biomass in boreal forest from multi-temporal ERS-1/2 interferometry. *Fringe 99: Second International Workshop on ERS SAR Interferometry*. Noordwijk, The Netherlands: ESA Publications Division, ESTEC.
- Santoro, M., Askne, J., Smith, G., Dammert, P. B. G., & Fransson, J. E. S. (2000). Boreal forest monitoring with ERS coherence. *ERS-Envisat Symposium*. Noordwijk, The Netherlands: ESA Publications Division, ESTEC.
- Schwäbisch, M., & Geudtner, D. (1995). Improvement of phase and coherence map using azimuth prefiltering: examples from ERS-1 and X-SAR. In: *IGARSS'95* (pp. 205–207). Piscataway, NJ: IEEE.
- Smith, G., Dammert, P. B. G., & Askne, J. (1996). Decorrelation mechanisms in C-Band SAR interferometry over boreal forest. In: G. Franceschetti, C. J. Oliver, F. S. Rubertone, & S. Tajbakksh (Eds.), *Microwave Sensing and Synthetic Aperture Radar. Proc. SPIE 2958* (pp. 300–310) Bellingham, Washington, USA.
- Smith, G., Dammert, P. B. G., Santoro, M., Fransson, J. E. S., Wegmüller, U., & Askne, J. (1998). Biomass retrieval in boreal forest using ERS and JERS SAR. *2nd International Workshop on Retrieval of Bio- and Geophysical Parameters from SAR data for Land Applications* (pp. 293–300). Noordwijk, The Netherlands: ESA Publications Division, ESTEC.
- Söderberg, U. (1986). Functions for forecasting of timber yields—increment and form height for individual trees of native species in Sweden. Report 14, Department of Forest Mensuration and Management, Swedish University of Agricultural Sciences, Umeå, Sweden.
- Wagner, W., Vietmeier, J., Schmullius, C., Davidson, M., Le Toan, T., Quegan, S., Yu, J. J., Luckman, A., Tansey, K., Balzter, H., & Gaveau, D. (2000). The use of coherence information from ERS tandem pairs for determining forest stock volume in SIBERIA. *IGARSS 2000* (pp. 1396–1398). Piscataway, NJ: IEEE.